

LONGITUDINAL HEAT CONDUCTION IN FINNED-TUBE EVAPORATORS

P.A. DOMANSKI^(a), J. M. CHOI^(b), W. V. PAYNE^(c)

^(a,c)National Institute of Standards and Technology, 100 Bureau Drive, Mail Stop 8631
Gaithersburg, Maryland 20899, USA, ^(a)e-mail: piotr.domanski@nist.gov

^(b)Department of Mechanical Engineering, Hanbat National University
16-1, Duckmyoung-Dong, Yuseong-Gu, Daejeon, 305-719, Korea

ABSTRACT

The paper evaluates performance of finned-tube evaporators at different refrigerant exit superheats to assess the impact of longitudinal heat conduction on capacity. A combination of capacity measurements obtained from laboratory testing, the pattern of measured return bend temperatures, and the theoretical analysis suggests the occurrence of tube-to-tube transfer via fins and rejects the tube longitudinal heat transfer as the possible causes of capacity degradation. The impact of tube-to-tube heat transfer was negligible in tests with a uniform 5.6 °C superheat, but it was significant in tests involving 16.7 °C superheat. The measured difference in capacity between two evaporators – in one of which tube-to-tube heat transfer was prevented by cuts in common fins – was as much as 23 %. The level of capacity degradation was affected by air volumetric flow rate.

1. INTRODUCTION

The general theory states that if a temperature gradient exists in a wall of a heat exchanger, then conduction heat transfer will occur along that wall and may degrade the performance of the heat exchanger. Kays and London (1984) identified the following three major parameters affecting the magnitude of performance degradation due to this phenomenon:

$$\lambda = \frac{kA_w}{LC_{\min}}, \quad \frac{C_{\min}}{C_{\max}}, \quad \text{and NTU} \quad (1)$$

The magnitude of the performance degradation becomes larger with increasing λ , C_{\min}/C_{\max} , and NTU. Kays and London stated that this reduction in performance is seen in heat exchangers designed for high effectiveness ($\epsilon > 0.9$), however, they did not provide a detailed quantitative analysis. Ranganayakulu et al. (1996) carried out a series of finite element simulations to quantify the magnitude of this performance degradation. The results of their simulations are represented by the “conduction effect factor”, τ , in terms of effectiveness with and without longitudinal conduction effects, ϵ_{WC} and ϵ_{NC} , respectively.

$$\tau = \frac{\epsilon_{NC} - \epsilon_{WC}}{\epsilon_{NC}} \quad (2)$$

The conduction effect factor can be read from the charts presented in the paper for given $\epsilon, \lambda, C_{\min}/C_{\max}$, and NTU. Ranganayakulu et al. suggested 0.8 as the effectiveness limit below which the impact of longitudinal conduction is negligible.

Heun and Crawford (1994) performed an analytical study of the effects of longitudinal fin conduction on a multipass cross-counterflow, single-depth-row heat exchanger. They considered the fins to have one-dimensional temperature distributions and solved them using a system of non-dimensional differential equations. Their results showed that longitudinal fin conduction always degrades heat exchanger performance, and this effect is stronger for a low normalized fin resistance and large values of the ratio of air-side conductance to air heat capacity.

Romero-Mendez et al. (1997) studied analytically tube-to-tube heat transfer by conduction through fins in a single-row finned-tube heat exchanger. They identified four non-dimensional groups that affected the degradation of evaporator capacity. The study indicated that tube-to-tube heat transfer always degrades capacity and that the influential parameters they identified have a non-linear impact on capacity degradation over the wide range of values studied. For some parametric values, they found the degradation to be as high as 20 %.

Asinari et al. (2004) developed a model for three-dimensional simulation of microchannel heat exchangers using a hybrid finite-volume and finite element discretization technique. Based on their simulations of supercritical carbon dioxide microchannel gas coolers they concluded that the heat conduction in fins in the direction of air flow and the longitudinal conduction in microchannel extrusions produced a negligible effect on the gas cooler performance.

Our literature review did not locate an experimental research study that would quantify the impact of longitudinal heat conduction in the heat exchanger material on heat exchanger capacity. In this paper we are attempting to do so based on previous measurements (Payne and Domanski, 2003).

2. EXPERIMENTAL SETUP AND TEST PROGRAM

Experimental Setup

Figure 1 shows a schematic diagram of the experimental setup located in the environmental chamber. The test rig consisted of three major flow loops: (1) a refrigerant vapor-compression loop, (2) a chilled water flow loop used for rejecting heat from the high-pressure refrigerant, and (3) an air flow loop used to supply heat to the tested evaporator. The refrigerant loop included a variable-speed compressor, water-cooled refrigerant condenser and subcooler, and three expansion valves to control refrigerant flow to the independent circuits of the evaporator. The design of the rig allowed independent control of operating parameters such as condensing pressure and subcooling at the inlet of the expansion valve (evaporator inlet enthalpy), pressure and superheat at the exit of the evaporator, and the exit superheats at the three individual evaporator circuits. A detailed description of the rig and methods for controlling different refrigerant parameters is presented by Payne and Domanski (2003).

Evaporator capacity was calculated using the air enthalpy method and refrigerant enthalpy method following procedures specified in ASHRAE Standard 37 (1998). The maximum difference between the air and refrigerant side capacity was less than 5 %. For a 95 % confidence level, the uncertainty in the evaporator capacity was also less than 5 % (Payne and Domanski, 2003).

We tested three evaporators, which were custom built for our study. The common design features they shared were: 3 depth rows with 18 tubes per row, tubes located in three parallel refrigerant circuits, 9.5 mm outside diameter 457.2 mm long round copper tubes, 25.4 mm tube spacing in a row, 0.11 mm thick aluminum fins. The following are differences between the tested evaporators along with their designated names:

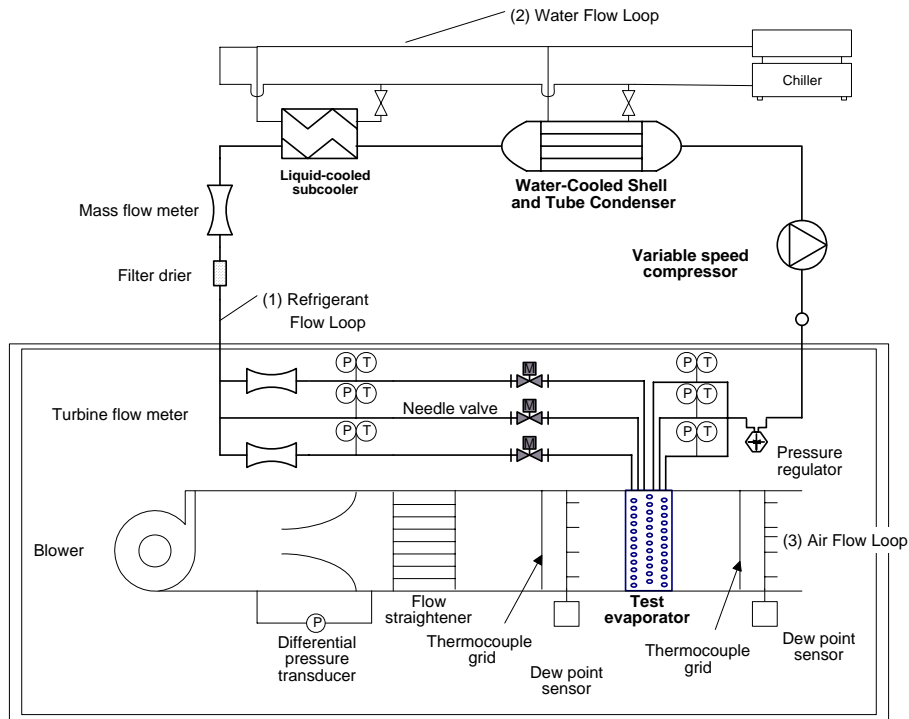


Figure 1. Schematic diagram of the experimental setup

- HX-wavy: used wavy fins; shown in Figure 2.
- HX-slit: the same as HX-wavy except for using slit fins instead of wavy fins
- HX-slit-cut: had the tube depth rows separated by a cut in fins; otherwise used the same slit fins as HX-slit; shown in Figure 3.

The heat exchangers were installed in the test tunnel to obtain cross-counter flow heat transfer between the air and refrigerant. Selected return bends of the evaporators were instrumented with thermocouples secured with copper tape, plastic “zip” ties, and foam insulation tape. The standard uncertainty of the bend temperature measurement was estimated to be 0.5 °C.



Figure 2. HX-wavy evaporator



Figure 3. HX-slit-cut evaporator

Table 1. Exit refrigerant superheat control for individual evaporator tests

Test #	Air Volumetric Flowrate (m ³ /h)		Overall Exit Superheat (°C)		
			Superheat in Individual Three Circuits (°C)		
	1300	1700	5.6	16.7	5.6
			5.6/5.6/5.6	16.7/16.7/16.7	Flooded/16.7/16.7
1	x		x		
2	x			x	
3	x				x
4		x	x		
5		x		x	

Test Conditions

We conducted all tests at $26.7\text{ °C} \pm 0.3\text{ °C}$ air dry-bulb temperatures and at $15.8\text{ °C} \pm 0.3\text{ °C}$ dew point. The refrigerant saturation temperature at the evaporator exit was maintained at $7.2 \pm 0.5\text{ °C}$. The refrigerant state at the inlet of expansion valves was controlled to maintain an enthalpy equivalent to a $48.9\text{ °C} \pm 1.4\text{ °C}$ saturation temperature with a subcooling of $8.3\text{ °C} \pm 1.4\text{ °C}$. Table 1 presents other operating variables controlled during the six different tests reported here. The unique aspect of our tests was the control of the overall evaporator superheat with individual control of the superheats at different circuit exits.

The most challenging conditions were those of Test 3, the overall superheat of 5.6 °C was obtained with 16.7 °C superheat at two circuit exits while the third circuit exit was being flooded. The specified superheats were obtained within 0.5 °C of the target values shown in Table 1.

3. EXPERIMENTAL RESULTS

Figure 4 shows HX-wavy bend temperature data for Test 1 (5.6 °C superheat on all circuits) and Test 3 (flooded top circuit with 16.7 °C superheat on the other two circuits). The Test 1 data show a uniform temperature distribution between comparable bends in the three refrigerant circuits. The noticeable difference occurs for Test 3 where the top circuit shows bend temperatures in the 9 °C to 10 °C range throughout all of its tubes, while the middle and bottom circuits show superheats at the third and fourth final tube bends with temperatures above of 21 °C . It is interesting to notice that the three last temperature readings for the bottom circuit show consecutively increasing temperatures (21.9 °C , 22.1 °C , and 23.2 °C) while the temperatures for the middle circuit do not increase (24.0 °C , 22.3 °C , 22.3 °C) but they rather drop at the location close to the flooded, low-temperature top circuit. It is reasonable to speculate that this temperature drop is a result of heat transfer via fins between the superheated tubes and the closely located flooded tubes with an approximate temperature of 9.2 °C .

Figure 5 shows capacities obtained on HX-slit and HX-slit-cut during tests with uniform individual superheats of 5.6 °C and 16.7 °C . The two evaporators had similar capacities during the tests with a 5.6 °C superheat (Tests 1 and 4); HX-slit-cut produced just slightly higher capacities than HX-slit possibly because of the added fin leading edges agitating the air boundary layer and increasing the air-side heat transfer coefficient. However, during the tests with 16.7 °C superheat (Tests 2 and 5), HX-slit-cut had significantly higher capacity than HX-slit. Since the two evaporators were of the same

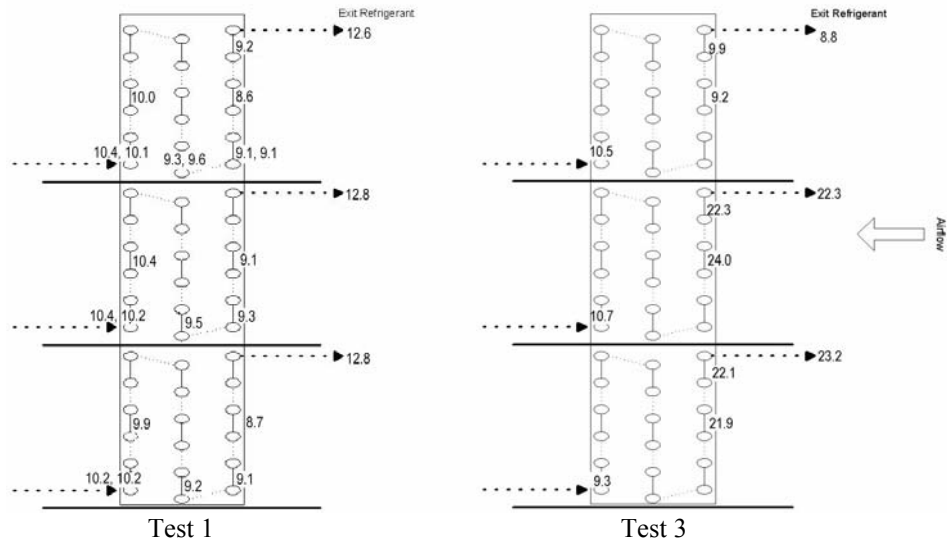


Figure 4. HX-wavy return bend temperatures for Test 1 (5.6/5.6/5.6 °C superheat) and Test 3 (flooded circuit/16.7/16.7 °C superheat).

design and materials other than the fin cut in HX-slit-cut, we can conclude that the reason for better performance of HX-slit-cut during tests with 16.7 °C superheat were the cut in fins, which eliminated the possibility of heat transfer via fins between tubes in the neighboring depth row.

Figure 5 also shows that the capacity difference between HX-slit and HX-slit-cut is greater at Test 5 (23 %) than at Test 2 (10 %); i.e., the superiority of HX-slit-cut is more pronounced at a higher volumetric flow of air. Since increasing the air flow increased the value of the C_{min} and C_{max} ratio, our result appears to be consistent with Ranganayakulu *et al.* (1997) who identified $C_{min}/C_{max} = 1$ as the value for the parameter at which the effect of longitudinal heat conduction may become significant.

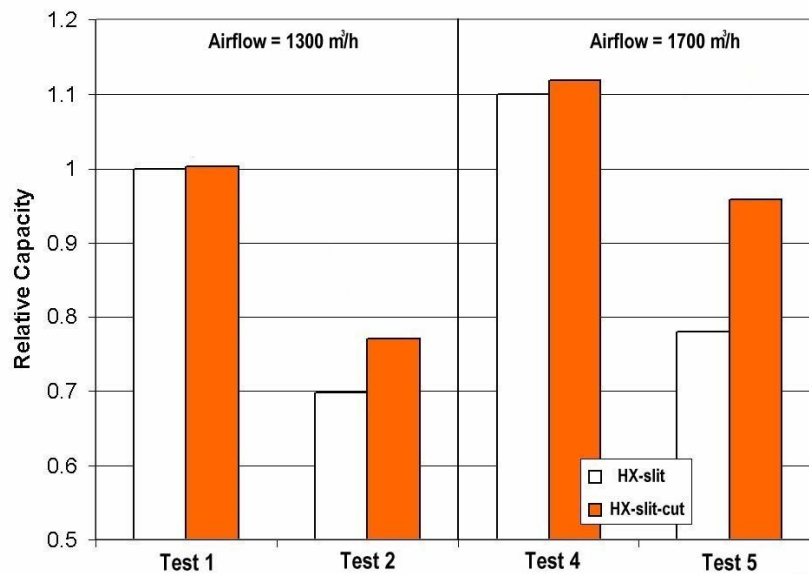


Figure 5. HX-slit and HX-slit-cut capacities at tests with 5.6 °C uniform superheat (Tests 1 and 4) and tests with 16.7 °C uniform superheat (Tests 2 and 5) relative to HX-slit capacity at Test 1

The occurrence of heat transfer between neighboring tubes in HX-slit can also be deduced from examining return bend temperatures for HX-slit and HX-slit-cut for Test 1 (5.6 °C superheat) and Test 2 (16.7 °C superheat). Figure 6 shows that the two evaporators have comparable bend temperatures during Test 1. For Test 2 with a 16.7 °C superheat (Figure 7), the average refrigerant inlet temperature for HX-slit was higher than that for HX-slit-cut by over 2 °C (9.4 °C versus 11.7 °C). Since the refrigerant saturation temperature at the evaporator exit was 7.2 °C for all tests, it follows that HX-slit had a higher refrigerant pressure drop than HX-slit-cut in spite of having a lower refrigerant mass flow than HX-slit. We can explain this apparent contradiction by the internal heat transfer within HX-slit contributing to an increase of refrigerant quality in the middle-depth-row tubes, which enhanced the pressure drop. We may further notice that the second-to-last return bend for each circuit in HX-slit registered an approximately 1.5 °C higher temperature than a corresponding return bend in HX-slit-cut, which also supports the conclusion on the contribution of tube-to-tube heat transfer to increasing refrigerant quality in middle-depth-row tubes.

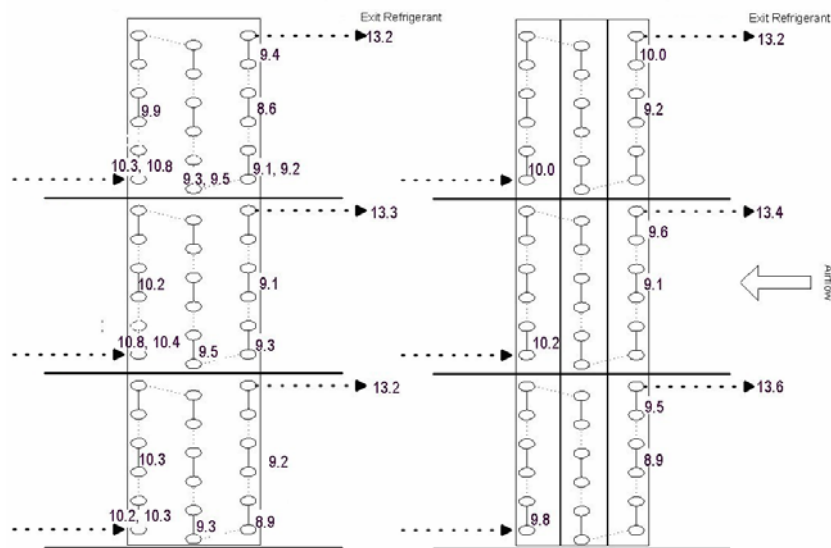


Figure 6. HX-slit and HX-slit-cut return bend temperatures for Test 1 (5.6 °C superheat on all circuits)

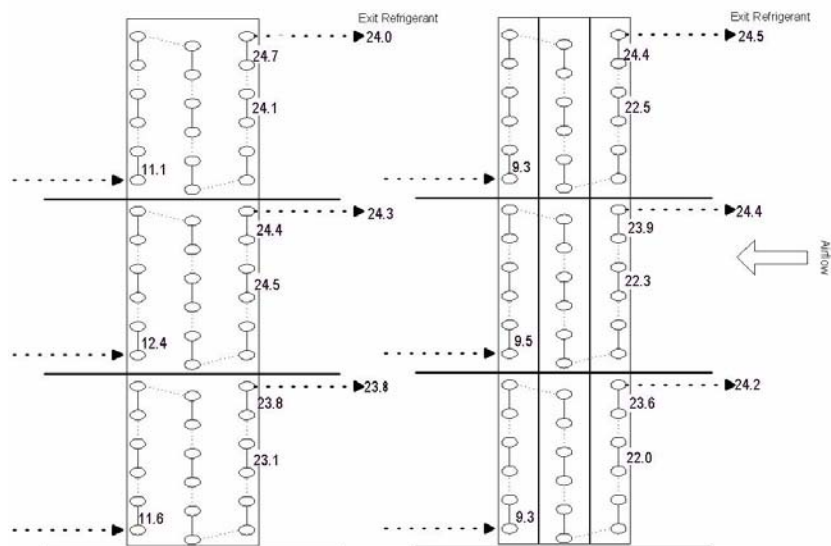


Figure 7. HX-slit and HX-slit-cut return bend temperatures for Test 2 (16.7 °C superheat on all circuits)

4. DISCUSSION

Internal heat transfer in a finned-tube evaporator can occur in the form of longitudinal heat conduction via tubes or fins. To find out the relative contributions of these two phenomena, we used a finned-tube simulation model, EVAP-COND (NIST, 2006) to simulate a 5 kW finned-tube evaporator and identify the tubes with superheated vapor, in which longitudinal heat conduction could take place. For the evaporator exit superheat of 8.0 °C, the simulations showed that only 5 of the 48 tubes in the heat exchanger had superheated refrigerant and experienced a meaningful temperature change (drop of saturation temperature due to the pressure drop was neglected). One of the tubes with superheated vapor had the following values for the parameters aforementioned in Equation (1).

$$\lambda = \frac{kA_w}{LC_{\min}} = 0.0011 \qquad \frac{C_{\min}}{C_{\max}} = 0.411 \qquad \text{NTU}=0.368$$

These parameters lie below the range of data given by Ranganayakulu *et al.* (1996). Using extrapolation, it was determined that the conduction effect factor would be approximately 0.0005. This means that this particular tube would see a loss in capacity of approximately one twentieth of one percent due to longitudinal tube conduction. When this capacity degradation was summed over all of the tubes in the heat exchanger where this effect occurs, the capacity reduction totaled only 0.13 W. It should be noted that the effectiveness of the example tube was 0.29. Hence, our result agrees with the general statements by Kays and London (1984) and that of Ranganayakulu *et al.* (1996) that the longitudinal tube heat conduction has an insignificant effect for heat exchangers with low effectiveness, below 0.9 and 0.8, respectively.

If we recognize that longitudinal tube heat conduction has a negligible impact, then the difference in capacities HX-slit and HX-slit-cut at 16.7 °C superheat must be due to longitudinal fin conduction. Our EVAP-COND simulation of HX-slit and HX-slit-cut pointed in this direction. EVAP-COND was able to predict capacities measured during tests with 5.6 °C uniform superheat within 5.1 % for all heat exchangers: however, for tests with 16.7 °C superheat EVAP-COND over-predicted HX-slit capacity by approximately 20 % while still being able to predict HX-slit-cut within 5 %. Since EVAP-COND does not account for the longitudinal fin heat transfer, it could predict well the performance of HX-slit-cut, in which internal heat transfer was minimized by cutting the fins between the depth rows, and substantially over-predicted the performance of HX-slit when internal heat transfer was significant.

5. CONCLUSIONS

We evaluated the performance of finned-tube evaporators at different refrigerant exit superheats to assess the impact of longitudinal heat conduction on capacity. A combination of capacity measurements obtained from laboratory testing, the pattern of measured return bend temperatures, and the theoretical analysis suggests the occurrence of tube-to-tube heat transfer via fins and rejects the tube longitudinal heat transfer as the possible causes of capacity degradation. The impact of tube-to-tube heat transfer was negligible in tests with a uniform 5.6 °C superheat, but it was significant in tests involving 16.7 °C superheat. The measured difference in capacity between two evaporators – in one of which tube-to-tube heat transfer was prevented by cuts in common fins – was as much as 23 %. The level of capacity degradation was affected by the air volumetric flow rate.

NOMENCLATURE

A_w - cross-sectional area perpendicular to flow (m^2)	<i>Subscripts</i>
C - product of mass flow rate and specific heat at constant pressure ($W K^{-1}$)	f - fin
k - thermal conductivity ($W m^{-1} K^{-1}$)	max - maximum
L - length of flow channel or distance between centers of adjacent tubes (m)	min - minimum
NTU - number of transfer units	NC - no conduction
P - pressure (kPa)	WC- with conduction
T - temperature (K)	<i>Greek Characters</i>
HX-wavy - evaporator with wavy fins	λ - flow factor from Kays and London (1984)
HX-slit - evaporator with slit fins	ε - heat exchanger effectiveness
HX-slit-cut - evaporator with cut slit fins to inhibit heat transfer	τ - conduction effect factor from Ranganayakulu <i>et al.</i> (1996)

ACKNOWLEDGEMENT

The paper has been derived from the project report ARTI-21CR/605-20050-01 entitled "Potential Benefits of Smart Refrigerant Distributors" sponsored by the Air-Conditioning and Refrigeration Technology Institute under its "HVAC&R Research for the 21st Century" (21-CR) Program. The funding for this 21-CR project was provided by the U.S. Department of Energy under Cooperative Agreement No DE-FC05-99OR22674; the Air-Conditioning and Refrigeration Institute; the Copper Development Association; the New York State Energy Research and Development Authority; the Refrigeration Service Engineers Society; and the Heating Refrigeration Air Conditioning Institute of Canada.

REFERENCES

- Asinari, P., Cecchinato, L., Fornasieri, E., 2004, Effects of thermal conduction in microchannel gas coolers for carbon dioxide, *Int. J., Refrig.*, 27(6): 577-586.
- ANSI/ASHRAE Standard 37-1988, *Methods of testing for rating unitary air conditioning and heat pump equipment*. American Society of Heating, Refrigerating and Air-Conditioning Engineers. 1791 Tullie Circle NE, Atlanta, GA, USA.
- Heun, M.K., Crawford, R.R., 1994, Longitudinal Fin Conduction in Multipass Cross-Counterflow Finned-Tube Heat Exchangers, *ASHRAE Transactions*, 100(1): 382-389.
- Kays, W.M., London, A.L., 1984, *Compact Heat Exchangers*, McGraw-Hill.
- NIST. 2006. *EVAP-COND - Simulation models for finned-tube heat exchangers*, Version 2.2, National Institute of Standards and Technology, Gaithersburg, MD, USA.
<http://www2.bfrl.nist.gov/software/evap-cond/>
- Payne, W.V., Domanski, P.A., 2003, *Potential benefits of Smart Refrigerant Distributors*, ARTI-21CR/605-200-50-01, National Institute of Standards and Technology, Gaithersburg, MD.
- Ranganayakulu, Ch. et al. 1997, The effects of longitudinal heat conduction in compact plate-fin and tube-fin heat exchangers using a finite element method, *Int. J. Heat Mass Transfer*, 40(6): 1261-1277.
- Romero-Mendez, R., Sen, M., Yang, K.T., McClain, R.L., 1997. Effect of tube-to-tube conduction on plate-fin and tube heat exchanger performance, *Int. J. Heat Mass Transfer*, 40(16): 3909-3916.